

Opto-Electronics Review

OPTO-ELECTRONICS
REVIEW

W

No. 100 Aug. 13
HOWERS 4
2025

journal homepage: https://journals.pan.pl/opelre

Optimisation of optical frequency comb (OFC) generation using advanced modulation techniques: A comparative analysis

Jeyapiriya K *0, Baskaran M 0

Department of Electronics and Communication Engineering, Sri Sairam Engineering College, Chennai, India

Article info:

Article history:
Received 28 May 2025
Received in revised form 23 Aug. 2025
Accepted 30 Aug. 2025
Available on-line 20 Oct. 2025

Keywords:
OFC;
Mach-Zehnder modulator;
frequency modulator;
phase modulator;
polarisation modulator;
dual drive Mach-Zehnder modulator.

Abstract

Optical frequency combs (OFCs) have transformed metrology, optical communications, and high-precision spectroscopic applications. OFC technology has advanced quickly over the last 20 years, placing it at the forefront of optical engineering and laser research. High-quality and stable OFCs are produced using sophisticated modulation techniques that effectively mould the comb spectral properties. Four important modulation strategies for OFC generation are compared in this study: Mach-Zehnder modulation (MZM), frequency modulation (FM), phase modulation (PM), and polarisation modulation (PolM). Two important factors of OFC namely, comb flatness and the number of lines generated are used to assess these modulators performance. The results of experiments and simulations show the benefits and drawbacks of each method and offer guidance on their optimal use in various optical systems. The results of this study provide a detailed understanding of the optimisation of OFC generation, which will aid in the creation of next-generation optical communication and sensor systems. Also, the various applications of OFC are discussed in the last section of this study.

1. Introduction

Specialised lasers known as optical frequency combs (OFCs) act as a kind of light ruler. They swiftly and precisely measure precise light frequencies, ranging from visible red, yellow, green, and blue light to invisible infrared and ultraviolet light. Scientists can measure and manipulate light waves as if they were radio waves using OFCs. Clocks, computers, and other devices that use radio or microwave frequencies can now be easily connected to optical waves that oscillate at frequencies 10 000 times higher.

OFCs provide a degree of precision higher than any other measurement method by directly measuring the oscillations of light. Direct measurement characteristics is used in applications ranging from quantum computation to metrology [1] and the market and number of OFC manufacturing companies are growing, as is the user community. The technique known as OFCs finds use in many different fields, mainly because of its accurate and reliable frequency references. In domains such as atomic and molecular spectroscopy [2], OFCs provide highly precise frequency references that allow

for reliable measurements. Applications like finding fundamental constants and deepening our knowledge of quantum systems depend on this technique. Timekeeping has been revolutionised using OFCs [3]. They make it possible to produce extremely steady optical frequencies, which are useful for making extremely precise optical clocks. These optical clocks are more accurate than conventional microwave frequency atomic clocks [4]. High-resolution spectroscopy is made possible by OFCs, which offer a dense collection of regularly spaced frequency lines.

OFCs make it easier to precisely identify molecular species using spectroscopic techniques in domains such as biology and chemistry. This has applications in material characterisation, medical diagnostics, and environmental monitoring. Frequency combs can be used for coherent communication in optical communication systems [5]. They make it possible to create several wavelength channels, which facilitates the efficient use of the optical spectrum and high-capacity data transmission [6]. In communication networks [7], OFCs can be used to establish precise time references, which will improve synchronisation and boost data transmission efficiency overall.

^{*}corresponding author at: priyainchrist@gmail.com

Ultra-fast laser pulses [8] are produced by OFCs. Applications for these pulses include materials processing, attosecond physics, and non-linear optics. Broadband optical spectra, such as those produced by frequency combs, are useful for a number of purposes, such as material characterisation and optical coherence tomography (OCT), a medical imaging technique. Astronomical spectrographs [9, 10] use OFCs to accurately characterise starlight. This aids in the search for exoplanets and contributes to our understanding of the universe. OFCs are helpful for space-based communication [11, 12] search work has been done in the generation of OFC.

Thus, OFCs have become invaluable tools with applications in spectroscopy, quantum technologies, telecommunications, and precision metrology. OFCs act as a foundation that unites several scientific and technical fields. This study focuses on the four important modulation strategies of OFC generation, namely Mach-Zehnder modulation (MZM), phase modulation (PM), frequency modulation (FM), and polarisation modulation (PolM), and a comparative analysis is performed on the results generated using these methods.

2. Fundamental principles of OFCs

OFCs act as exact rulers in the optical frequency domain as shown in Fig. 1. These are produced by specialised laser [13] and are vital instruments in many high-precision fields, including metrology, spectroscopy, and telecommunications. A laser [14] typically has a natural bandwidth that is influenced by the optical cavity and gain medium rather than just one wavelength or frequency. The light waves in the optical cavity will interfere with one another both destructively and constructively, forming a configuration of standing waves. Longitudinal modes are the distinct frequency sets that characterise standing waves, as shown in Fig. 2. The only frequencies of light that the resonant cavity permits to oscillate independently are these modes.

The output of a laser has several thousands of modes. As a result, the output intensity will always remain the same; this is referred to as a continuous wave (CW). A CW laser will periodically interfere with itself if all of its modes are fixed in phase relationship. Consequently, the laser generates light pulse trains and is referred to as mode-locking technology [15] . Through the fixing of the relative phases of each longitudinal lasing mode, mode-locked lasers [16] produce ultra-short optical pulse trains that are repeated over time [17, 18]. The time interval τ_c between these pulses is provided by (1) [19]:

$$f_s = \frac{2L}{v},\tag{1}$$

where L is the length of the cavity and v is the speed of light in vacuum. In the frequency domain, OFC is seen as a pulse of equally spaced lines with the optical frequency at its center given by (2) [20]:

$$f(p) = f_c + p \cdot f_s,\tag{2}$$

where p denotes the integer, f_s is the comb spacing and f_c is the carrier frequency. Early attempts to construct such OFCs were based on heavily driven electro-optic (EO) mod-

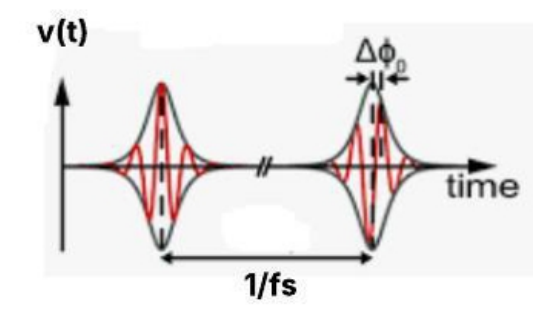


Fig. 1. OFC in time domain.

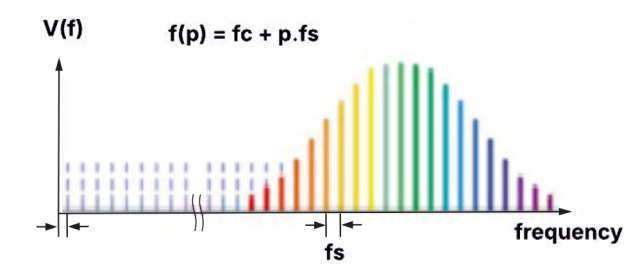


Fig. 2. OFC in frequency domain.

ulators [21,22], which may impose thousands of sidebands on a single-frequency input beam from a single-frequency CW laser.

3. Experimental techniques for OFC generation

OFC creation provides a way to increase data speeds and spectral efficiency. To produce OFCs, several experimental methods have been devised; each has special benefits and uses. Various general methodologies used to create OFCs are tabulated in Table 1, which briefly describes the methodology involved in each type with examples, their advantages and disadvantages.

Although every method presents specific benefits—like increased efficiency, broad bandwidth, compactness, or adaptability—it also comes with its own set of disadvantages, including complexity, low efficiency, or limited bandwidth. Overall, Table 1 provides a comparative overview of the different methods for generating OFCs, which are crucial for applications in spectroscopy, precision metrology, and advanced communication systems. The following sections concentrate on OFC generation using different configurations implementing MZM, FM, PM, and PolM.

3.1. Generation of OFC using Mach-Zehnder modulator (MZM)

An apparatus that modifies the phase or intensity of an optical wave by means of the EO effect [23] is called MZM [24].

PM is introduced to an incoming optical signal when it is driven by an electrical signal, as shown in Fig. 3. Sidebands surrounding the carrier frequency can be produced by adjusting the modulation settings [31]. MZM is an EO modulator in which the modulator arms refractive index varies in response to changes in the applied electric field. It consists of two waveguides that act as interferometer

Table 1 Types of generation of OFC.

TYPE 1	Mode-locked lasers	
Methodology	Evenly spaced OFCs are generated using	
- Italiodologj	mode-locked lasers	
Example	Ti:Sapphire mode-locked lasers, Erbium-doped fiber lasers	
Advantages	High coherence and stability, broad bandwidth [25]	
TYPE 2	Electro-optic modulation (EOM) comb generation	
Methodology	Uses EOMs driven by radio frequency (RF) to form sidebands around a carrier generated by CW laser [26]	
Example	Phase and intensity modulators	
Advantages	Highly tunable comb spacing, compact and stable	
Disadvantages	Limited bandwidth	
TYPE 3	Kerr microresonators	
Methodology	Kerr non-linear high-Q microresonators are used to generate OFCs via four-wave mixing (FWM) [27]	
Example	Chip-based microresonators	
Advantages	Energy-efficient, CMOS-compatible	
Disadvantages	Requires precise dispersion engineering and pump power control	
TYPE 4	Supercontinuum generation in non-linear fibres [28,29]	
Methodology	Ultra-fast laser with high-power is injected into a non-linear fibre, generating a broad OFCs	
Example	Photonic crystal fibres (PCFs)	
Advantages	Ultra-broadband combs covering visible to mid-infrared	
Disadvantages	Requires high-power lasers and careful dispersion control	
TYPE 5	Parametric comb generation	
Methodology	OFCs are produced by non linear frequency conversion using optical parametric oscillators (OPOs)	
Example	Second order non-linear crystals	
Advantages	Widely tunable and broad spectral coverage	
Disadvantages	Requires phase-matching conditions	
TYPE 6	Raman and Brillouin Combs [30]	
Methodology	Uses stimulated Raman or Brillouin scattering to generate frequency combs	
Advantages	Can be generated in standard fibres	

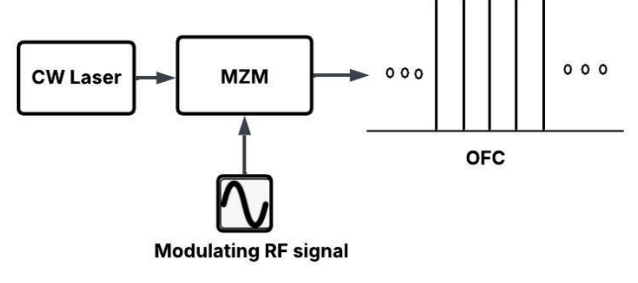


Fig. 3. Generation of OFC using MZM.

arms. The input waveguide, to which the laser is attached, is split into two channels, each of which has electrodes surrounding it. Because of the shift in refractive index caused by the electrodes connection to the modulated signal voltage and direct current (DC) bias voltage, each arm refractive index is altered, resulting in PM. By connecting the interferometer arms, the PM [32] is ultimately converted to intensity modulation (IM). By adjusting the sidebands power deviation, the IM non-linear effect [33] flattens the comb lines at the MZM output. The electric field expression of the input optical signal [34] is expressed in (3):

$$E_{\text{input}} = E_m \cos(\omega t \pm \phi),$$
 (3)

where ω is the frequency and ϕ is the phase of the input signal. The output optical signal obtained at the output of the modulator [34] is represented as (4):

$$E_{\text{output}}(t) = E_{\text{input}} \cos (\omega t \pm \phi),$$
 (4)

where

$$\phi = \phi_{\text{initial}} + \Delta \phi_{\text{c}}$$
.

 ϕ represents the phase shift of the modulated signal, ϕ_{initial} is the initial phase, and $\Delta\phi_{\text{c}}$ is the change in phase due to modulation. This change in phase can be written as in terms of electric field of modulating signal as:

$$\Delta\phi_c = (\pi/\lambda)n_r^3 r x V,$$

where x is the length of the EO material of width w, n_r is the non-linear refractive index and V is the electric field generated around the EO material due to applied modulating signal. By neglecting the constant phase term and applying the identity, the output of modulated light wave becomes (5):

$$E_{\text{output}} = E_a(J_0(m)\cos(\omega t) + J_1(m)\cos(\omega + \omega_m)t$$

$$-J_1(m)\cos(\omega - \omega_m)t$$

$$+J_2(m)\cos(\omega + 2\omega_m)t - \cdots).$$
(5)

The function $J_n(m)$ is defined as the n^{th} -order Bessel function. The carrier with an amplitude of $J_0(m)$ and a series of sidebands symmetrically spaced at frequency separations of ω_m , $2\omega_m$, $3\omega_m$, $4\omega_m$, etc. constitute the spectrum. The Bessel function of first type and order n is denoted by the function $J_n(m)$. The Bessel function $J_n(m)$ determines the amplitude of the spectral components and is shown in Fig. 4.

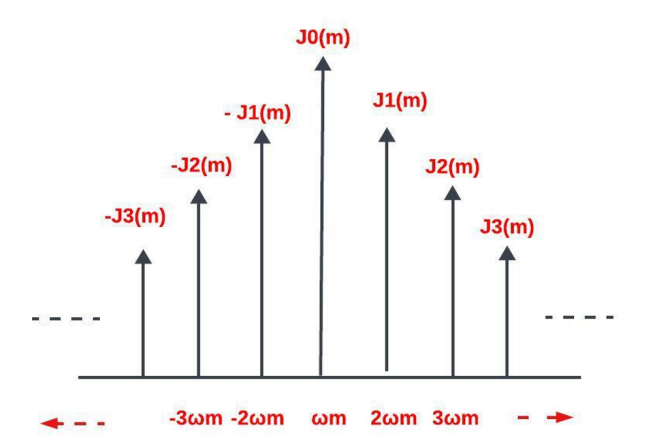


Fig. 4. Frequency comb represented using Bessel function.

3.1.1. OFC generation using dual electrode MZM (DE-MZM)

The cascaded structure of MZM [35] as shown in Fig. 5 increases the comb lines. Here, the two stages of DE-MZM proposed by Kun generate 16 comb lines [36]. The first stage generates 4 comb lines. When these comb lines [37] act as carriers to the second stage, a total of 16 comb lines are produced. Kun performed his analysis in Optisystem software considering a wavelength of the CW laser to be 1552.52 nm of 10 dBm power and a line width of 100 kHz. The half-wave voltage to the modulator is 3 V with an extinction ratio of 20 dB [38]. The RF frequency of the first modulator, MZM1 is taken as 16 GHz with 24.08 dBm power and the RF frequency of second modulator, MZM2 is 4 GHz with 12.04 dBm power. With these specifications, Kun was able to achieve 4 comb lines in the output of the first MZM1 and 16 comb lines in the output of MZM2 with the characteristic parameters stated in Table 2.

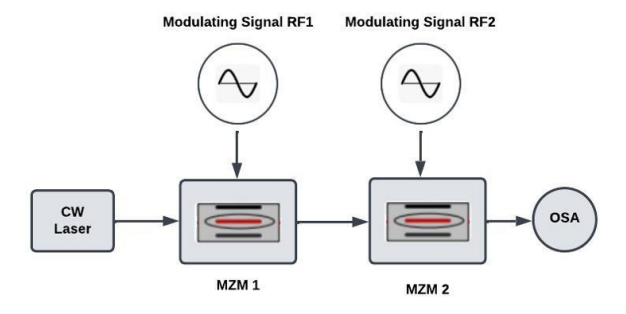


Fig. 5. Two stage cascaded structure of DE-MZM.

Characteristics	Stage 1	Stage 2
RF (GHz)	16	4
Number of comb lines	4	16
Frequency spacing (GHz)	32	8
UMSR (dB)	16.5	16.5
Comb flatness (dB)	0.25	0.48

Here, the flatness of the frequency comb is maintained when there is a drift in the bias voltage of MZM [39]. For MZM1, the flatness is maintained at 0.53 dB for a bias drift of ± 4 %. The same performance is evident for a bias drift of ± 10 %. Taking into account MZM2, the flatness is maintained at 0.54 dB for a bias drift of ± 4 % and also for a drift of ± 10 %. When both MZMs are considered, the flatness is maintained to be 0.48 dB for a bias drift of ± 4 % and 0.55 dB flatness and 15.9 dB unwanted modes suppression ratio (UMSR) [40,41] for a bias drift of ± 10 % which is tabulated in Table 3.

Table 3
Influence of bias drift on flatness.

COMB FLATNESS		
Experimental setup	Bias drift of -4% and +4%	Bias drift of -10% and +10%
With MZM1	0.53	0.53
With MZM2	0.54	0.54
With MZM1 and MZM2	0.48	0.55

3.1.2. Generation of OFC using DA-MZM

Hraghi *et al.* use a single DA-MZM [42] in his setup. DC bias is applied to the DA-MZM. $X_1(t)$ and $X_2(t)$ are the sinusoidal RF signals applied to MZM as shown in Fig. 6. DC bias induces phase shift of θ_1 and θ_2 with A_1 and A_2 being the amplitude of $X_1(t)$ and $X_2(t)$, respectively. The flatness condition of Sakamoto *et al.* [43] is used as in (6) to (8):

$$X_1(t) = A_1 \sin \omega_1 t \tag{6}$$

$$X_2(t) = A_2 \sin \omega_2 t \tag{7}$$

$$\Delta A \pm \Delta \theta = \pi/2,\tag{8}$$

where $\Delta A = (A_1 - A_2)/2$ is the peak to peak phase difference $\Delta \theta = (\theta_1 - \theta_2)/2$ is the DC bias difference of the two arms of the modulators and $A_{\rm av} = (A_1 + A_2)/2$ is the average amplitude.

The output spectrum based on the above flatness condition produces 11 comb lines with a comb flatness of 1.1 dB.

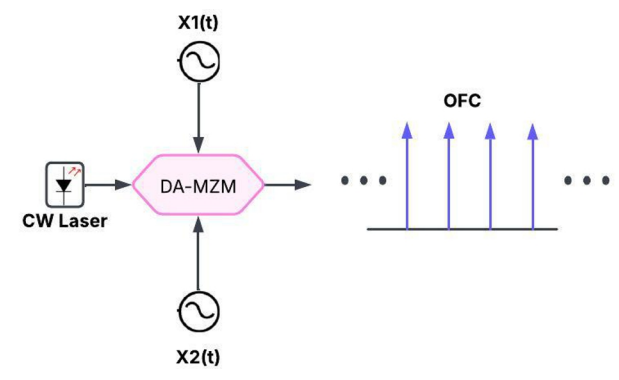


Fig. 6. Optical flat comb generation based on DA-MZM.

3.1.3. Generation of OFC using cascaded structure of two dual arm (DA-MZM) and push pull MZM

It is a useful instrument in optical communication systems due to its dual drive structure, which allows for fine control over the generated comb lines. The dual drive MZM [44] generates numerous comb lines by modulating the optical carrier with two RF impulses.

The setup implemented by Hraghi [42] consists of DA-MZM cascaded with push pull MZMs shown in Fig. 7. Two sine waves given in (6) and (7) are excited synchronously to DA-MZM. The push pull MZM is excited by a sinusoidal signal of $S_3(t) = A_3 \sin \omega 2t$. Assuming that the phase of the source is zero, the output spectrum was obtained according to (9) which is the expression of the n^{th} -order harmonic envelope:

$$E_{\text{output}}[n] = \frac{1}{2} |E_{\text{in}}| \sum_{k=-\infty}^{+\infty} J_k(A_1) J_{n-k}(A_3)$$

$$\times \left[e^{j\theta_1} + e^{j((n-k)\pi - (\theta_3 - \theta_1))} \right] + J_k(A_2) J_{n-k}(A_3)$$

$$\times \left[e^{-j\theta_2} + e^{j((n-k)\pi - (\theta_3 + \theta_2))} \right].$$
(9)

Hraghi proposed a new optimisation method in his work considering the following conditions:

- i. Generate maximum number of flat optical comb harmonics for a particular ripple value.
- ii. Consider the normal range of operation of driving signals.
- iii. To obtain the nominal flatness coefficient, equation (10) must be satisfied.

$$\theta \max \left| \|C\|^2 - \bar{RP} \right| \le \Delta R \quad \forall k \in \left[-\frac{N}{2}, \frac{N}{2} \right],$$

$$\theta \min \left| \|C\|^2 - \bar{RP} \right| > \Delta R \quad \text{otherwise.}$$
(10)

Here, ΔR is the allowed ripple, j is the spectrum region that produces a flat response. By means of a linear search, the different regions are found on the vector $C = [\ldots, C_k, C_{k+1}, \ldots]$. Simulated annealing algorithm is applied as an optimisation algorithm for the large search space. The author proposed a new condition given in (11) to generate flatness in the frequency comb [45]:

$$\Delta A \pm \Delta \theta = \pm m \cdot \frac{\pi}{4}.\tag{11}$$

In a single stage, MZM modulator is shown in Fig. 6. 4, 8, 16, and 32 new spectral lines are obtained with P = 1 dB, in addition to the center wavelength of 1552.52 nm.

In a two stage of MZM, 41 spectral lines are obtained with 1 dB as comb flatness using the optimised algorithm proposed in [46]. The modulation frequency is 12.5 GHz.

3.1.4. Generation of OFC using cascaded intensity and dual parallel MZM (DP-MZM)

Zhou achieved 20 lines frequency comb using a structure consisting of two intensity modulators cascaded with a DP-MZM [47]. The comb lines generated are flat with 0.6 dB comb flatness. The first stage consists of 2 MZMs in a cascade [48] fashion driven by an RF frequency f. The CW laser [49] was modulated by one MZM. Keeping the DC bias of MZM1 to zero, carrier and even sidebands are obtained in the output spectrum. Then, when the bias of MZM2 is set as π , it produces a double sideband with suppression modulation. Two synchronised signals are applied to DP-MZM with frequency f_2 applied to the upper arm and $2f_2$ applied to the lower arm shown in Fig. 8.

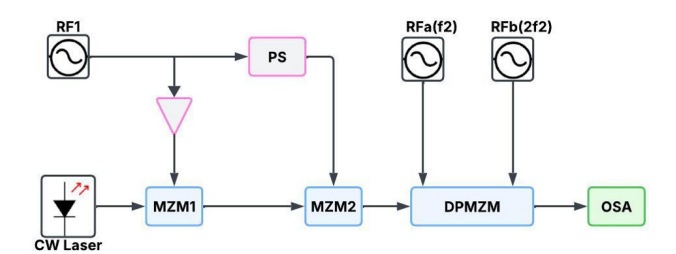


Fig. 8. Cascaded structure of MZM and DP-MZM.

The modulation index is defined by (12):

$$m = V_{RF}/V_{\pi}. \tag{12}$$

Here, V_{RF} is the applied voltage and V_{π} is the half-wave voltage of the MZM. For MZM1, keeping m=1.55, $f_1=25$ GHz, 4 spectral lines are obtained as the output of stage 1 with 0.2 dB comb flatness and frequency separation of 50 GHz. The other spectral lines are suppressed at 22 dB. By proper bias adjustments to MZM, 20 OFC lines with a comb flatness of 0.6 dB were achieved.

The number of comb lines can be increased by applying more power of the applied RF signal to DP-MZM [50] and also they can be increased by adding more modulators [51]. The other undesirable frequency sideband lines are present in the output spectrum because of the limitations of the extinction ratio present in the modulator [52].

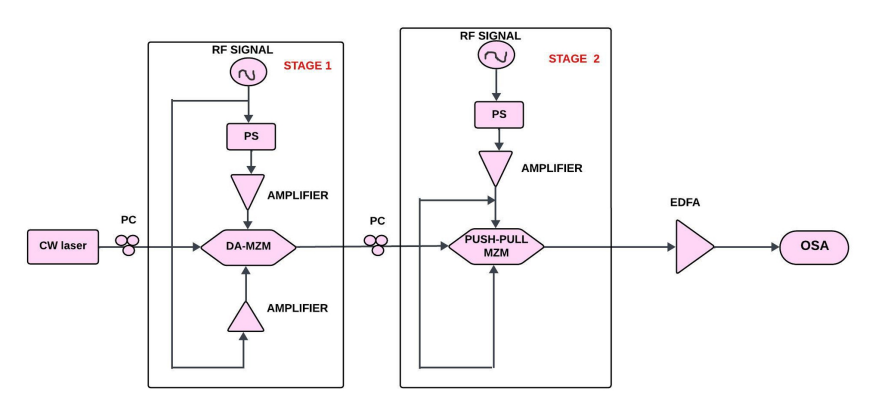


Fig. 7. Cascaded strucutre of DA-MZM and push pull MZM.

3.2. Generation of OFC implementing only phase modulations (PMs)

In [53], PMs in a cascade fashion were implemented to obtain a higher modulation index, which in turn increased the number of spectral lines compared to the use of electrical amplifiers [54,55]. The following sub-sections explain two different structures with 2 and 3 PMs [56].

3.2.1. Generation of OFC using PMs in cascade fashion

The system consists of two stage PM namely PM1 and PM2. The first stage can be used with more than one PM. A CW light wave is applied to the first stage of this structure. A phase shifter is implemented in the first stage between the modulators so that the driving signals are synchronous in Fig. 9.

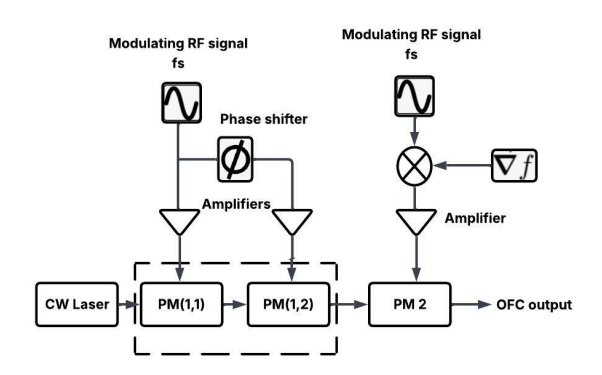


Fig. 9. Structure of two stage PMs.

When the phase difference ϕ is averaged, a flattened output is obtained by adjusting the two parameters, the PM indices m_1 and m_2 . The comb flatness becomes larger than 10 dB when there is no frequency offset. The following results are observed for the setup implemented with two PMs in cascade:

- i. Phase deviation has no impact on the flatness of the comb.
- ii. Comb lines of 21 carriers are generated with less than 3 dB flatness.
- iii. To generate the flatness to be less than 3 dB, the frequency offset is found to be higher than $1 \times 10^{-5} f_s$. Then the output of the frequency comb [47] is given by (13):

$$E_{\text{output 1}}(t) = E_c \exp\left[j\pi R_1 \sin\left(2\pi f_s t\right)\right]$$
$$= E_o \sum_{n=-\infty}^{\infty} J_n \left(\pi R_1\right) \exp\left[j2\pi \left(f_c + n f_s\right) t\right],$$
(13)

where J_n is the first-order Bessel function and m is the modulation index [57]. Setting the frequency offset to zero, the driving signal for the second stage PM2 is expressed as in (14):

$$f_2(t) = m_2 V_{\pi} \sin(2\pi f_s t + \phi)$$
. (14)

Here, ϕ is the fixed phase difference between the driving RF signals of the first and second stage. The output after PM2 [58] is:

$$E_{\text{output}}(t) = E_c \exp\left[j\pi m_c \sin\left(2\pi f_s t + \psi\right)\right], \qquad (15)$$

where m_c is the combined modulation index as shown in (16), and

$$m_c = \sqrt{m_1^2 + 2m_1 m_2 \cos \phi + m_2^2}. (16)$$

3.2.2. Generation of OFC using 3 PMs

Experimental setup consists of 3 PMs [43] called PM1, PM2, and PM3 shown in Fig. 10. These 3 stages are implemented in 2 stages with 2 modulators in the first stage and 1 PM in the last stage. They are driven by an RF frequency signal of 25 GHz frequency. The half-wave voltage of 4 V is amplified to 13 V by an electrical amplifier. The insertion loss is set to 4 dB. The modulation index is found to be 3.25 in the first stage. The number of frequency lines has been increased by driving the second stage PM modulator with a frequency offset of 500 kHz, the RF frequency being 25 000 GHz with a peak voltage of 3.6 V. Here, the modulation is set to 0.45. Thus, with the introduction of small frequency offset, 21 comb lines can be generated with comb flatness less than 3 dB.

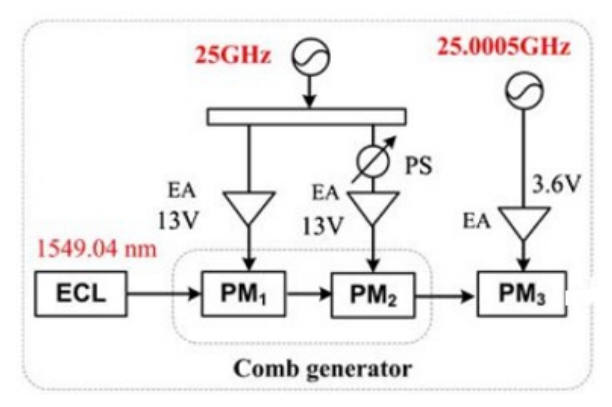


Fig. 10. Structure of three stage PMs.

The spectrum of the comb is produced after the first stage of phase modulation without frequency offset. 19 comb lines with a frequency spacing of 25 GHz are produced with a flatness greater than 18 dB. At 25 GHz frequency spacing, approximately 21 lines are produced. These OFCs have a reduced flatness of less than 3 dB.

3.3. Generation of OFC using cascaded FM and MZM

Laser source is cascaded with a single-drive MZM and 2 FMs [59]. By adjusting or modifying the parameters of an FM [60], the system can generate the desired OFC. RF impulses with sinusoidal frequencies of f_m , $f_{m/2}$, and 2 f_m , respectively, power the modulators. As seen in Fig. 11, there is no need for an amplifier or phase shifter because each of the modulators receives the RF signal directly. As a result, the design is straightforward, reliable, and power-efficient. The following is a description of all the device specifications mentioned in Table 4.

- i. First set of RF1, RF2, and RF3 signals: 16 GHz, 8 GHz, and 32 GHz.
- Second set of RF1, RF2, and RF3 signals: 8 GHz, 4 GHz and 16 GHz.

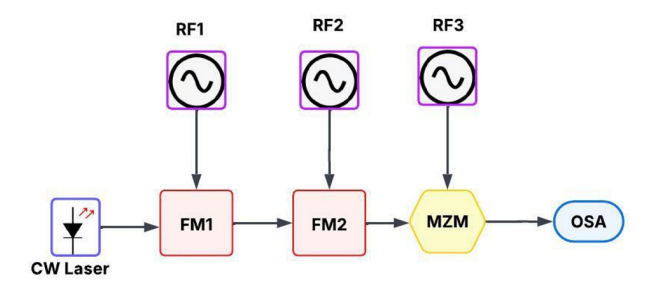


Fig. 11. Structure of the system model with cascaded FM and MZM.

Table 4 Specifications of the system model.

S.no	Parameters of the modulators	Values
1.	Frequency deviation	10 GHz
2.	Bias voltage 1	-2.8 V
3.	Bias voltage 2	-1.1 V
4.	Modulation voltage	15 V
5.	Laser power	1 mW
6.	Line width	10 MHz
7.	Centre frequency	193.1 THz
8.	Amplitude of RF 1 signal	2 a.u.
9.	Amplitude of RF 2 signal	2 a.u.
10.	Phase of RF 1 signal	90°
11.	Phase of RF 2 signal	45°

The first FM generates the subcarriers, while the second FM increases the number of comb lines mentioned in Table 5.

Table 5Output of the system model.

Parameters	First FM	Second FM
Comb lines for $f_m = 16 \text{ GHz}$	19	37
Comb lines for $f_m = 8 \text{ GHz}$	38	71
Sub-carrier spacing for $f_m = 16 \text{ GHz}$	16 GHz	8 GHz
Sub-carrier spacing for $f_m = 8 \text{ GHz}$	8 GHz	4 GHz
Flatness	≤ 1 dB	≤ 2dB

3.4. OFC generation using PolMs

The fundamental concept is to create sidebands that resemble a comb-like spectrum by combining a PolM with a polariser and PM effects. A PolM is a unique type of EOM that has the ability to phase modulate two orthogonal polarisation components at the same time. A bias voltage is not necessary for a PolM to function, in contrast to a traditional PM or intensity modulator (IM). Both input laser polarisation components are modulated by the PolM [61]. Multiple sidebands are produced by the PM effect that the RF signal

generates. The phase components interfere when they are sent through a polariser, producing an output that is varied in intensity. As a result, the OFC has an interval equal to the frequency of the RF drive. Benefits include high sideband generation efficiency, bias-free operation (no need for DC bias), and adjustable comb spacing through RF driving frequency adjustment. Unlike other non-linear comb generation methods [62, 63], it is compact and stable.

3.4.1. OFC generation using PolM and frequency shifter with double recirculating frequency shifting loops

A PolM and a complementary frequency shifter are employed in the two stage procedure described in the investigation to create ultraflat and stable OFCs [64,65].

The first step is to use a PolM to create a five-carrier light source. The ensuing frequency-shifting process is sparked by this light source. The PolM [66] is driven by a radio frequency component (RF1), two polarisation controllers (PCs), a polariser (Pol), and an external cavity laser (ECL). To produce the necessary polarisation states, the light from the ECL is oriented at a particular angle to the PolM shown in Fig. 12.

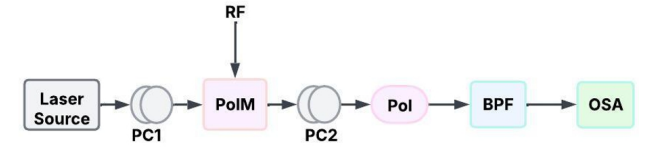


Fig. 12. OFC generation using PolM.

The polarisation-modulator-based complementary frequency shifter (PCFS), which is intended to do frequency shifting without the requirement for DC bias control, is then fed the produced five-carrier light source. Compared to traditional approaches, which usually require these controls, this is a major improvement. By using a dual-recirculation frequency shifter (RFS) arrangement [67] with polarisation-maintained optical coupler (PMOC) [68] as shown in Fig. 13, the PCFS makes it possible to generate numerous frequency lines via a recirculating loop. To make sure that only the desired frequency components are kept, light is amplified and modulated before being filtered using an optical bandpass filter (BPF). The approach places a strong emphasis on optimising a number of factors, such as modulator drive voltage, filter stop-band attenuation, and optical amplifier gain.

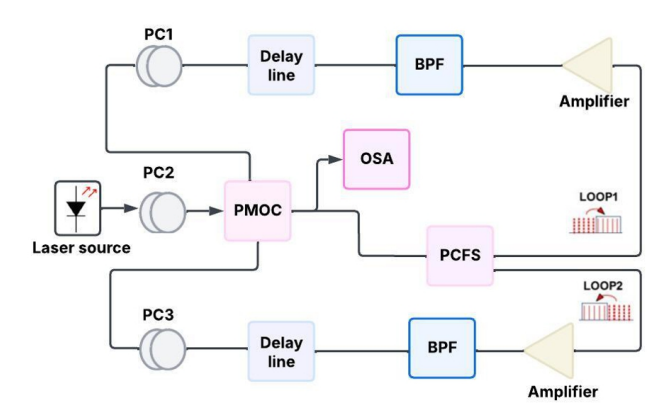


Fig. 13. Structure of dual-RFS arrangement with PMOC.

For the resulting OFC to be as flat and stable as possible, several optimisations are essential. The trials demonstrated the efficacy of the suggested method by demonstrating that a high-quality OFC with hundreds of frequency lines and minimum comb flatness below 2 dB could be created by modifying these parameters.

To illustrate the effectiveness of the suggested OFC generating strategy, the technique consists of both theoretical simulations and experimental validations. The findings demonstrate the method resilience with a tone-noise ratio (TNR) of 38 dB and a frequency spacing of 12.5 GHz. This thorough approach demonstrates the novel features of the suggested system, which greatly improves OFC creation while lowering complexity and noise.

3.4.2. OFC generation using a polarisation division multiplexing MZM (PDM-MZM)

The methodology for creating OFCs using a PDM-MZM is shown in Fig. 14. The OFC is generated by a single PDM-MZM which in turn is made of 2 MZMs [69]. In contrast to conventional techniques, which frequently require several devices, this innovative method seeks to generate more comb lines with higher spectral flatness. A CW laser source that produces an optical carrier with a wavelength of 1550 nm is part of the experimental setup. This light is introduced into the PDM-MZM, which is made up of 2 sub-MZMs, a polarisation beam combiner (PBC), and a polarisation beam splitter (PBS). Complementary intensity modulation along orthogonal polarisation directions is possible with the PDM-MZM. RF impulses are applied to the sub-MZMs in order to modulate the optical signal. The first sub-MZM RF frequency is configured to produce the first comb lines, and

the second sub-MZM is powered by an RF signal that is either one-ninth or nine times the first frequency, which enables the creation of more comb lines. Another PDM-MZM is cascaded as part of the process to further expand the number of comb lines. The initial comb lines produced by the first modulator can be enlarged through this cascading process, yielding 81 comb lines with a spectral comb flatness of less than 1.6 dB. In order to attain the required spectrum flatness and stability, the methodology highlights the significance of modifying a number of factors, including the modulator modulation indices and DC bias points. The success of the optimisation procedure was demonstrated by the testing findings, which displayed a spectrum comb flatness of 0.63 dB and an UMSR of 17.5 dB.

3.4.3. Polarisation-dependent high-quality OFC generator based on RFS

The paper novel approach to creating a polarisation-dependent OFC includes a number of crucial elements and procedures.

Using a DP-MZM [60] to perform carrier-suppressed single sideband (CS-SSB) modulation forms the basis of the suggested method implemented in Fig. 15. In order to create the first frequency comb lines, this modulation approach is essential. DP-MZM [70] can effectively manipulate the optical signal since it operates in two orthogonal polarisations [71].

To produce a five-line OFC, a polarisation modulator [65, 72] is incorporated into the system. By working with the DP-MZM, the PolM makes it possible to use polarisation multiplexing [73] to create numerous frequency lines. This two-pronged strategy improves the comb generating process overall productivity and efficiency.

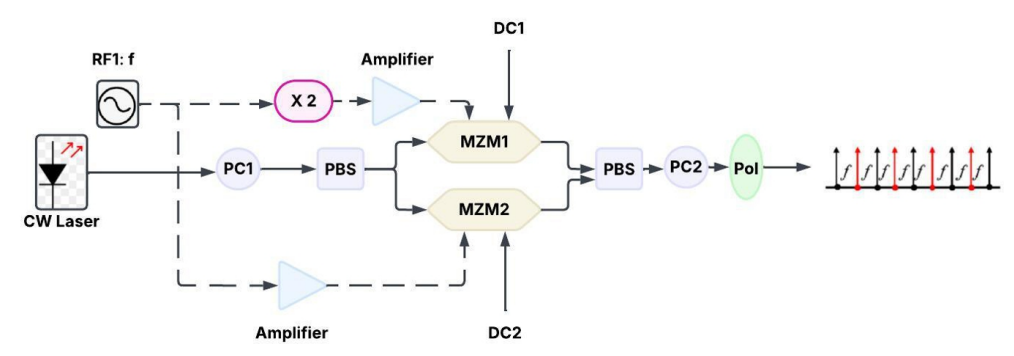


Fig. 14. OFC generator based on a PDM-MZM.

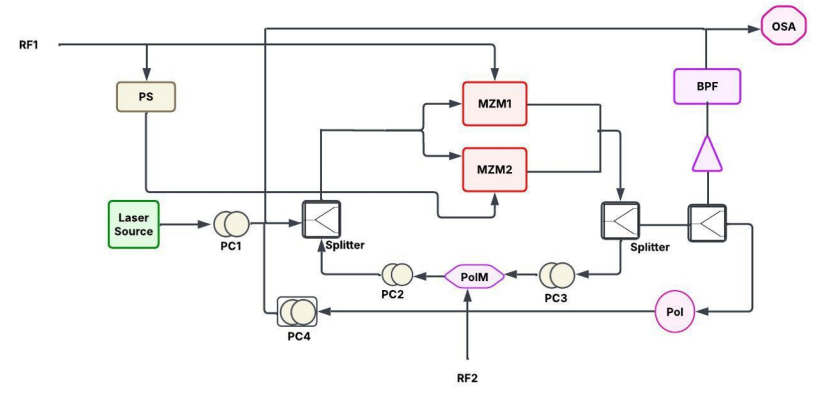


Fig. 15. Structure of the system model with polarisation modulator and MZM.

An RFS mechanism is incorporated into the process, which is crucial to increase the number of frequency lines generated. This method produces a wider and more stable OFC output by recirculating and shifting the generated frequency components. Simulation data are included in the research to show how effective the suggested methodology is. The simulations demonstrate the potential for high-quality comb creation by showing that the technique can produce a 120-line OFC with a flatness of 3.91 dB. The outcomes demonstrate how well the method works to produce a flat and steady frequency comb. The technique has a strong emphasis on optimising a number of factors, including the alignment of the optical components and the modulation depth. Achieving the intended performance criteria, such as output power stability and spectral flatness, depends on these optimisations. This thorough process demonstrates the creative features of the suggested OFC generating approach, which uses cuttingedge modulation methods and polarisation control to provide excellent outcomes.

3.5. OFC generation using CMOS-compatible cascaded MZM

This process creates OFCs with excellent tunability and integration potential by using MZMs EOM capabilities [74]. Multiple comb lines with controlled spacing and amplitude fluctuations can be generated using cascaded MZMs, making it appropriate for a variety of applications, such as metrology and optical communications [75]. Cascaded MZMs, which are integrated on silicon-on-insulator (SOI) platforms, show promise for small, on-chip solutions by producing dual-wavelength combs with 9 lines and 10 GHz spacing. In silicon photonics, quasi-rectangular OFCs with 9 lines and a comb spacing of up to 10 GHz can be created using two cascaded EO MZMs while preserving amplitude variation within 6.5 dB [76,77].

The application of cascaded MZMs in silicon photonics has been shown to produce quasi-rectangular OFCs with certain properties [78]. The creation of OFCs with a high degree of tunability in terms of central frequency and comb spacing is made possible by the use of cascaded MZMs in silicon photonics [76]. This is essential for a number of applications, including metrology and optical communications. With a comb spacing of up to 10 GHz and 9 lines, the exhibited system can generate OFCs while keeping the amplitude fluctuation within 6.5 dB. Using CMOS cascaded MZM, the frequency spacing and output power with deviations obtained are tabulated in Table 6

4. Performance evaluation of different OFC methods

From detailed examinations of the different methods of OFC generation done in the previous sections, the summary is tabulated in Table 7. Two important features are targeted in these generation methods: the number of comb lines generated and the flatness in the power of the output spectrum [79]. Each design aims to increase the efficiency of the combs, but maintaining flatness with an increased number of comb lines remained difficult, but this problem was solved by increasing the number of modulators in cascade fashion. A detailed investigation of the Table 7 shows that with DE-MZM archi-

Table 6Output of the system design.

Frequency spacing (GHz)	Output power (dBm)	Power deviation
5	-28.6	3.8
7.5	-26.8	4.7
10	-28.5	6.5

Table 7

Analysis of different methodologies of generating OFC using modulators.

Section no.	OFC generation methodology	No. of comb lines	Power flatness (dB)
3.1.1	DE-MZM	16	0.48
3.1.2	DA-MZM	11	1.1
3.1.3	Cascaded DA-MZM and push pull MZM	41	1
3.1.4	Cascaded intensity and DP-MZM	20	0.6
3.2.1	Cascaded 2 PMs	21	less than 3
3.2.2	Cascaded 3 PMs	21	less than 3
3.3	Cascaded FM and MZM	37	less than 2
3.4.1	PM and frequency shifter	55 and 105	36 and 33
3.4.2	PDM- MZM	81	less than 1.6
3.4.3	DP-MZM and PolM	120	3.91
3.5	CMOS compatible cascaded MZMs	9	6.5

tecture, 16 comb lines are produced with power flatness as good as 0.48 dB. Considering the structure with DP-MZM and PolM, an increased number of comb lines of about 120 lines was generated but the power flatness is not that desirable, which is of 3.91 dB. Similarly, other methods are tabulated. Thus, a trade-off is to be made between these two parameters.

5. Applications, challenges and future directions of OFCs

This section highlights the milestones reached by researchers in the field of OFCs over the past two decades. Table 8 shows the timeline of research achievements in this area. In addition, OFCs can form a single source for WDM systems that provides high data rates with low error rates required for 5G applications [80,81]. Satellite networks are increasingly using OFC technology to improve communication efficiency and capacity. OFC integration is essential for contemporary satellite communication systems because it enables high-speed data transfer, flexible spectrum allocation, and improved error correction. OFC greatly increases data capacity

 Table 8

 Yearwise significant advancement of OFCs.

Duration	Technological development of OFCs	
1999	Theodor Hänsch and John Hall were granted the Nobel Prize in Physics in recognition of their contributions to the advancement of laser-based precision spectroscopy, which served as the foundation for OFCs.	
2000- 2004	First type of OFCs with frequency stabilisation and mode-locked lasers.	
2005	Creating an OFC in a microresonator.	
2007	Albert Fert and Peter Grünberg were given the Nobel Prize in Physics for their discovery of enormous magnetoresistance, which aided in the development of magnetic sensors that are frequently employed with OFCs.	
2008	Microcomb and fibre-based combs.	
2009	OFC start to find application in metrology, telecommunication, and optical clocks.	
2013	OFC integrated with photonic devices.	
2015	Extension to new domains like environmental sensing, quantum computing, and astronomy.	
2018	OFC in quantum communication systems.	
2021	On-chip OFC integration with silicon photonics.	

in satellite networks by enabling optical wireless communication (OWC) systems that can reach bidirectional transmission rates of up to 90 Gbps over 5000 km distances [82]. Optical satellite networks architecture enables connections without pre-deployed equipment and instantly adjusts to traffic volumes and atmospheric conditions [83]. Researchers use OFCs to effectively analyse human breath [84]. Current available techniques for identifying minute amounts of chemicals in breath are either unwieldy, slow, sensitive only to particular molecules, incompetent in differentiating between several compounds, or imprecise in determining their concentrations [85]. The researchers were able to identify certain molecules [86] and their quantities by identifying which hues of light were absorbed and in what amounts—basically, searching for light absorbed close to the "teeth" of the OFC. With great precision, frequency resolution, and sensitivity, researchers can evaluate a wide range of potential chemical compounds simultaneously using the optical comb technique [87]. But the approach is still in its early stages of research only. From 1999, great interest has developed towards the generation of OFC, the advancements are depicted in Table 8. OFCs can identify particular molecules as simple as carbon dioxide and complex antibodies. They provide results with exceptional accuracy. OFCs can also be used to detect COVID in the breath [88]. Researchers at the University of Colorado, Toptica Photonics AG, and the National Institute of Standards and Technology (NIST) have now created an OFC that can identify molecules in a sample in a billionth of a second. In order to identify the colour spectrum that a molecule absorbs, the researchers employed the widely used dual-OFC arrangement [89], which consists

of two laser beams that cooperate. Most dual frequency comb configurations use two femtosecond lasers [90] that pulse twice as quickly as each other. Future nanometer-level measurements of far-off satellites may be made possible by this invention, and the team is also investigating the potential benefits of its time-programmable OFC for other comb sensing applications [91]. Molecular spectroscopy and trace gas detection, combs for astronomy, optical frequency division, WDM [92], quantum control, optical communications, biophotonics, quantum information processing [93], characterisation and time/frequency dissemination of optical clocks, microwave photonics [94], etc. are the various applications of the OFC.

6. Conclusions

This study compares Mach-Zehnder, frequency, phase, and polarisation modulators for OFC creation, emphasising their individual benefits and drawbacks. The findings show that every modulation method has different properties with respect to stability, power efficiency, comb flatness, and spectral bandwidth. FM and PM improve spectral purity, PolM allows more degrees of freedom for comb shaping, and MZM provides high tunability. The particular application requirements, such as broad coverage for optical communications [95] or strong spectral coherence for metrology, decide on the selection of the modulation scheme. The performance of OFC-based systems can be greatly enhanced by refining these modulation techniques, opening the door to developments in next-generation photonic technologies, precise measurement, and high-speed optical networks. The integration of data from multiple studies highlights the critical role OFCs play in improving a variety of technological sectors as scientists continue to investigate new directions and improve current methods.

In summary, this study provides an extensive resource for researchers, engineers, and hobbyists on the subject by compiling a plethora of information on the fabrication of OFCs using various modulators. Future breakthroughs in OFC technology will undoubtedly influence precise measurement and optical communications, opening the door to revolutionary advances in science and technology.

Authors' statement

- 1. K. Jeyapiriya has done the conceptualisation, methodology, investigation, and writing the original draft.
- 2. M. Baskaran has done supervision, writing the review, editing, and validation. Both authors have read and approved the final manuscript.

References

- [1] Caldwell, E. D., Sinclair, L. C., Newbury, N. R. & Deschenes, J.-D. The time-programmable frequency comb and its use in quantum-limited ranging. *Nature* **610**, 667–673 (2022). https://doi.org/10.1038/s41586-022-05225-8.
- [2] Cruz, F. C. *et al.* Mid-infrared optical frequency combs based on difference frequency generation for molecular

- spectroscopy. *Opt. Express* **23**, 26814–26824 (2015). https://doi.org/10.1364/OE.23.026814.
- [3] Pasquazi, A. et al. Micro-combs: A novel generation of optical sources. Phys. Rep. 729, 1–81 (2018). https://doi.org/10.1016/j.physrep.2017.08.004.
- [4] Diddams, S. A. The evolving optical frequency comb. *J. Opt. Soc. Am. B: Opt. Phys.* 27, B51–B62 (2010). https://doi.org/10.1364/JOSAB.27.000B51.
- [5] Yang, K. Y. et al. Multi-dimensional data transmission using inverse-designed silicon photonics and microcombs. Nat. Commun. 13, 7862 (2022). https://doi.org/10.1038/s41467-022-35446-4.
- [6] Fischer, J. K. et al. Beyond 100g-high-capacity transport technologies for next generation optical core networks. In 2012 Future Network & Mobile Summit (FutureNetw), 1–9 (IEEE, 2012).
- [7] Baskaran, M. & Kishanlal, M. S. M. A novel DWDM-based comb source for future optical network. *J. Nonlinear Opt. Phys. Mater.* 33, 2350054 (2024). https://doi.org/10.1142/S0218863523500546.
- [8] Sun, D. *et al.* 10-GHz ultrashort pulse and flat optical comb generation via a semiconductor mode-locked laser. *SSRN* 1–13 (2025). https://doi.org/10.2139/ssrn.5084520.
- [9] Blind, N., Coarer, E. L., Kern, P. & Gousset, S. Spectrographs for astrophotonics. *Opt. Express* 25, 27341–27369 (2017). https://doi.org/10.1364/OE.25.027341.
- [10] Endo, M., Sukegawa, T., Silva, A. & Kobayashi, Y. Subgigahertz-resolution table-top spectrograph calibrated with a 4-GHz optical frequency comb. *J. Astron. Telesc. Instrum. Syst.* 6, 020501 (2020). https://doi.org/10.1117/1.JATIS.6.2.020501.
- [11] Lezius, M. et al. Space-borne frequency comb metrology. Optica 3, 1381–1387 (2016). https://doi.org/10.1364/OPTICA.3.001381.
- [12] Giunta, M. *et al.* Optical frequency combs for space applications. In *2016 Conference on Lasers and Electro-Optics (CLEO)*, 1–2 (IEEE, 2016). https://doi.org/10.1364/CLEO_SI.2016.STh4H.5.
- [13] Chen, Z. et al. Tunable optical frequency comb generated using periodic windows in a laser and its application for distance measurement. Sensors 23, 8872 (2023). https://doi.org/10.3390/s23218872.
- [14] Rosado, A. et al. Numerical and experimental analysis of optical frequency comb generation in gain-switched semiconductor lasers. IEEE J. Quantum Electron. 55, 1–12 (2019). https://doi.org/10.1109/JQE.2019.2943482.
- [15] Ye, J. & Cundiff, S. T. Femtosecond optical frequency comb: Principle, operation and applications (Springer Science & Business Media, 2005).
- [16] Sooudi, E. et al. Observation of harmonic-mode-locking in a mode-locked InAs/InP-based quantum-dash laser with CW optical injection. *IEEE Photonics Technol. Lett.* 23, 549–551 (2011). https://doi.org/10.1109/LPT.2011.2114338.
- [17] Jones, D. J. et al. Carrier-envelope phase control of femtosecond mode-locked lasers and direct optical frequency synthesis. Science 288, 635–639 (2000). https://doi.org/10.1126/science.288.5466.635.
- [18] Udem, T., Holzwarth, R. & Hänsch, T. W. Optical frequency metrology. *Nature* 416, 233–237 (2002). https://doi.org/10.1038/416233a.
- [19] Holzwarth, R. et al. Optical frequency synthesizer for precision spectroscopy. Phys. Rev. Lett. 85, 2264 (2000). https://doi.org/10.1103/PhysRevLett.85.2264.
- [20] Zhang, H. et al. Coherent optical frequency combs: from principles to applications. J. Electron. Sci. Technol. 20, 100157 (2022). https://doi.org/10.1016/j.jnlest.2022.100157.

- [21] Zhai, K., Wang, W., Zhu, S., Wen, H. & Zhu, N. Optical frequency comb generation based on optoelectronic oscillator and Fabry-Perot phase modulator. *IEEE Photonics J.* **15**, 1–5 (2023). https://doi.org/10.1109/JPHOT.2023.3323286.
- [22] Buscaino, B., Zhang, M., Lončar, M. & Kahn, J. M. Design of efficient resonator-enhanced electro-optic frequency comb generators. *J. Light. Technol.* 38, 1400–1413 (2020). https://doi.org/10.1109/JLT.2020.2973884.
- [23] Parriaux, A., Hammani, K. & Millot, G. Electro-optic frequency combs. Adv. Opt. Photonics 12, 223–287 (2020). https://doi.org/10.1364/AOP.382052.
- [24] Qu, K. et al. Ultra-flat and broadband optical frequency comb generator via a single Mach–Zehnder modulator. IEEE Photonics Technol. Lett. 29, 255–258 (2016). https://doi.org/10.1109/LPT.2016.2640276.
- [25] Rosado, A. et al. Experimental study of optical frequency comb generation in gain-switched semiconductor lasers. Opt. Laser Technol. 108, 542–550 (2018). https://doi.org/10.1016/J.OPTLASTEC.2018.07.038.
- [26] Fan, Y. & Shore, K. A. Generation of optical frequency combs using gain switched semiconductor nanolasers. *IEEE Photonics Technol. Lett.* 35, 713–716 (2023). https://doi.org/10.1109/LPT.2023.3274164.
- [27] Imai, K., Kourogi, M. & Ohtsu, M. 30-THz span optical frequency comb generation by self-phase modulation in an optical fiber. *IEEE J. Quantum Electron.* 34, 54–60 (1998). https://doi.org/10.1109/3.655007.
- [28] Bassiouni, M., Ismail, T., Selmy, H. & Badr, Y. Generation of ofc by self-phase modulation and multiple laser sources in HNLF. In 2020 16th International Computer Engineering Conference (ICENCO), 203–206 (IEEE, 2020). https://doi.org/10.1109/ICENCO49778.2020.9357325.
- [29] Weng, H.-Z. et al. Optical frequency comb generation in highly nonlinear fiber with dual-mode square microlasers. *IEEE Photonics J.* 10, 7102009 (2017). https://doi.org/10.1109/JPHOT.2017.2780280.
- [30] Ho, K.-P. & Kahn, J. M. Optical frequency comb generator using phase modulation in amplified circulating loop. *IEEE Photonics Technol. Lett.* 5, 721–725 (1993). https://doi.org/10.1109/68.219723.
- [31] Ullah, S. et al. Ultra-wide and flattened optical frequency comb generation based on cascaded phase modulator and LiNbO3-MZM offering terahertz bandwidth. IEEE Access 8, 76692–76699 (2020). https://doi.org/10.1109/ACCESS.2020.2989678.
- [32] Verma, P. & Singh, S. Exploiting cross-polarization modulation in semiconductor optical amplifier-Mach-Zehnder interferometer for enhanced optical frequency comb generation. *Opt. Eng.* 63 (2024). https://doi.org/10.1117/1.oe.63.11.115101.
- [33] Yang, T., Dong, J., Liao, S., Huang, D. & Zhang, X. Comparison analysis of optical frequency comb generation with nonlinear effects in highly nonlinear fibers. *Opt. Express* 21, 8508–8520 (2013). https://doi.org/10.1364/OE.21.008508.
- [34] Khalil, M., Sun, H., Papatheodorakos, T., Adams, R. & Chen, L. R. Optical frequency comb generation using integrated cascaded mzms on soi. In *2024 Photonics North (PN)*, 1–2 (2024).
- [35] Zhang, S. *et al.* Generation of a flat optical frequency comb via a cascaded dual-parallelMach-Zehnder modulator and phase modulator without using the fundamental tone. *Photonics* **10**, 1340 (2023). https://doi.org/10.3390/photonics10121340.

- [36] Qu, K., Zhao, S., Li, X., Tan, Q. & Zhu, Z. Ultraflat and broadband optical frequency comb generator based on cascaded two dual-electrode Mach–Zehnder modulators. *Opt. Rev.* 25, 264–270 (2018). https://doi.org/10.1007/s10043-018-0417-4.
- [37] Sakamoto, T., Kawanishi, T. & Izutsu, M. Widely wavelength-tunable ultra-flat frequency comb generation using conventional dual-drive Mach-Zehnder modulator. *Electron. Lett.* 43, 1 (2007). https://doi.org/10.1049/el;20071267.
- [38] Sun, H., Khalil, M., Wang, Z. & Chen, L. R. Recent progress in integrated electro-optic frequency comb generation. *J. Semicond.* 42, 041301 (2021). https://doi.org/10.1088/1674-4926/42/4/041301.
- [39] Nazneen, R. & Zahir, E. Analysis and optimization of an optical frequency comb for multiple channel transmission in a fiberoptic system. In 2016 3rd International Conference on Electrical Engineering and Information Communication Technology (ICEEICT), 1–4 (2016). https://doi.org/10.1109/CEEICT.2016.7873132.
- [40] Shang, L., Wen, A. & Lin, G. Optical frequency comb generation using two cascaded intensity modulators. *J. Opt.* 16, 035401 (2014). https://doi.org/10.1088/2040-8978/16/3/035401.
- [41] Deng, Z. et al. Ultra-precise optical phase-locking approach for ultralow noise frequency comb generation. Opt. Laser Technol. 138, 106906 (2021). https://doi.org/10.1016/j.optlastec.2020.106906.
- [42] Hraghi, A., Chaibi, M. E., Menif, M. & Erasme, D. Demonstration of 16QAM-OFDM UDWDM transmission using a tunable optical flat comb source. *J. Light. Technol.* 35, 238–245 (2017). https://doi.org/10.1109/JLT.2016.2636442.
- [43] Sakamoto, T. & Chiba, A. Multiple-frequency-spaced flat optical comb generation using a multiple-parallel phase modulator. *Opt. Lett.* 42, 4462–4465 (2017). https://doi.org/10.1364/OL.42.004462.
- [44] Li, W., Wang, W. T., Sun, W. H., Wang, L. X. & Zhu, N. H. Photonic generation of arbitrarily phase-modulated microwave signals based on a single DDMZM. *Opt. Express* 22, 7446–7457 (2014). https://doi.org/10.1364/OE.22.007446.
- [45] Sakamoto, T., Kawanishi, T. & Tsuchiya, M. 10 GHz, 2.4 ps pulse generation using a single-stage dual-drive Mach-Zehnder modulator. *Opt. Lett.* 33, 890–892 (2008). https://doi.org/10.1364/OL.33.000890.
- [46] Sakamoto, T., Kawanishi, T. & Izutsu, M. Optimization of electro-optic comb generation using conventional Mach-Zehnder modulator. In 2007 Interntional Topical Meeting on Microwave Photonics, 50–53 (IEEE, 2007). https://doi.org/10.1109/MWP.2007.4378133.
- [47] Zhou, X., Zheng, X., Wen, H., Zhang, H. & Zhou, B. Generation of broadband optical frequency comb with rectangular envelope using cascaded intensity and dual-parallel modulators. *Opt. Commun.* 313, 356–359 (2014). https://doi.org/10.1016/j.optcom.2013.10.054.
- [48] Wu, R., Supradeepa, V., Long, C. M., Leaird, D. E. & Weiner, A. M. Generation of very flat optical frequency combs from continuous-wave lasers using cascaded intensity and phase modulators driven by tailored radio frequency waveforms. *Opt. Lett.* 35, 3234–3236 (2010). https://doi.org/10.1364/OL.35.003234.
- [49] Malinowski, M., Rao, A., Delfyett, P. & Fathpour, S. Optical frequency comb generation by pulsed pumping. APL Photonics 2, 066101 (2017). https://doi.org/10.1063/1.4983113.

- [50] Huancachoque, L. A., dos Santos, M. L., Pereira, A. I., Nascimento, D. V. & Bordonalli, A. C. Optical frequency comb generation by dual drive Mach-Zehnder modulator with algorithm-assisted efficient amplitude equalization. In 2019 SBMO/IEEE MTT-S International Microwave and Optoelectronics Conference (IMOC), 1–3 (IEEE, 2019). https://doi.org/10.1109/IMOC43827.2019.9317691.
- [51] Jeyapiriya, K. & Baskaran, M. Generation of 103 ultra-flat broadband optical frequency comb lines using cascaded amplitude modulator and single drive Mach-Zehnder modulators. *J. Optoelectron. Adv. Mater.* 26, 368–375 (2024). https://joam.inoe.ro/articles/generation-of-103-.../.
- [52] Dou, Y., Zhang, H. & Yao, M. Generation of flat optical-frequency comb using cascaded intensity and phase modulators. *IEEE Photonics Technol. Lett.* 24, 727–729 (2012). https://doi.org/10.1109/LPT.2012.2187330.
- [53] Zhang, J. et al. Flattened comb generation using only phase modulators driven by fundamental frequency sinusoidal sources with small frequency offset. Opt. Lett. 38, 552–554 (2013). https://doi.org/10.1364/OL.38.000552.
- [54] Zhang, Y., Zhang, H. & Shu, C. Generation of optical frequency comb via cross-phase modulation in an SOI waveguide. In 2022 Optical Fiber Communications Conference and Exhibition (OFC), 1–3 (2022). https://doi.org/10.1364/OFC.2022.Tu3E.4.
- [55] Yan, J., Dong, H. & Wang, Y. Line-spacing-multiplied optical frequency comb generation using an electro-optic talbot laser and cross-phase modulation in a fiber. *Photonics* 11, 282 (2024). https://doi.org/10.3390/photonics11030282.
- [56] Supradeepa, V. R. & Weiner, A. M. Bandwidth scaling and spectral flatness enhancement of optical frequency combs from phase-modulated continuous-wave lasers using cascaded four-wave mixing. *Opt. Lett.* 37, 3066–3068 (2012). https://doi.org/10.1364/OL.37.003066.
- [57] Wang, M. & Yao, J. Tunable optical frequency comb generation based on an optoelectronic oscillator. *IEEE Photonics Technol. Lett.* 25, 2035–2038 (2013). https://doi.org/10.1109/LPT.2013.2280666.
- [58] Mohammadi, A. et al. High-repetition-rate electro-optic frequency combs using cascaded silicon phase modulators. Opt. Express 33, 23820–23834 (2025). https://doi.org/10.1364/OE.558298.
- [59] Ujjwal & Kumar, R. Optical frequency comb generator employing two cascaded frequency modulators and Mach-Zehnder modulator. *Electronics* 12, 2762 (2023). https://doi.org/10.3390/electronics12132762.
- [60] Cui, Y. *et al.* Flat optical frequency comb generation by using one DPMZM and superposed harmonics. *Opt. Commun.* **531**, 129223 (2023). https://doi.10.1016/j.optcom.2022.129223.
- [61] Lv, X. & Li, D. High-quality optical frequency comb generation-based on polarization modulator with RF frequency multiplication circuit and intensity modulator. *J. Opt. Commun.* 43, 347–352 (2022). https://doi.org/10.1515/joc-2019-0003.
- [62] Ricciardi, I. et al. Frequency comb generation in quadratic nonlinear media. Phys. Rev. A 91, 063839 (2015). https://doi.org/10.1103/PhysRevA.91.063839.
- [63] Ataie, V., Myslivets, E., Kuo, B. P.-P., Alic, N. & Radic, S. Spectrally equalized frequency comb generation in multistage parametric mixer with nonlinear pulse shaping. *J. Light. Technol.* 32, 840–846 (2014). https://doi.org/10.1109/JLT.2013.2287852.
- [64] Cui, Y., Li, R. & Wu, S. Flat optical frequency comb generation using polarization modulator and frequency shifter with double recirculating frequency shifting loops. *Opt. Quantum Electron.* 49, 338 (2017). https://doi.org/10.1007/S11082-017-1179-0.

- [65] Kageyama, T. & Hasegawa, T. Fast polarization control for optical frequency combs. *Opt. Express* 29, 38477–38487 (2021). https://doi.org/10.1364/OE.439346.
- [66] Verma, P. & Singh, S. An approach to generate cross-polarization modulation-enabled optical frequency comb with enhanced spectral flatness in traveling-wave semiconductor optical amplifiers. J. Opt. 26, 105703 (2024). https://doi.org/10.1088/2040-8986/ad6f24.
- [67] Li, R., Wu, S., Ye, S. & Cui, Y. Very flat optical frequency comb generation based on polarization modulator and recirculation frequency shifter. *J. Opt. Commun.* 39, 7–12 (2017). https://doi.org/10.1515/joc-2016-0108.
- [68] Li, D., Wu, S., Liu, Y. & Guo, Y. Flat optical frequency comb generation based on a dual-parallel Mach–Zehnder modulator and a single recirculation frequency shift loop. *Appl. Opt.* 59, 1916–1923 (2020). https://doi.org/10.1364/AO.381880.
- [69] Shang, L., Li, Y. & Wu, F. Optical frequency comb generation using a polarization division multiplexing Mach–Zehnder modulator. *J. Opt.* 48, 60–64 (2019). https://doi.org/10.1007/S12596-019-00516-2.
- [70] Wang, X., Wei, Y., Gong, C., Liu, S. & Fan, D. Optical frequency comb generation based on DPMZM cascades FM, EAM and PolM. In 2021 IEEE 6th Optoelectronics Global Conference (OGC), 56–60 (IEEE, 2021). https://doi.org/10.1109/OGC52961.2021.9654330.
- [71] Lin, T. *et al.* Polarization-dependent high quality optical frequency comb generator based on recirculating frequency shift. In *2018 Asia Communications and Photonics Conference (ACP)*, 1–3 (Optica Publishing Group, 2018). https://doi.org/10.1109/ACP.2018.8596266.
- [72] Guo, Y., Liu, Y., Li, D. & Wu, S. Ultra-flat optical frequency comb generation based on a polarization modulator and a butterworth band-stop filter. *Appl. Opt.* 60, 5540–5546 (2021). https://doi.org/10.1364/AO.424836.
- [73] Doumbia, Y., Wolfersberger, D., Panajotov, K. & Sciamanna, M. Tailoring frequency combs through vcsel polarization dynamics. *Opt. Express* 29, 33976–33991 (2021). https://doi.org/10.1364/OE.432281.
- [74] Xu, M. & Cai, X. Advances in integrated ultra-wideband electro-optic modulators. *Opt. Express* **30**, 7253–7274 (2022). https://doi.org/10.1364/OE.449022.
- [75] Paul, P. S., Sadia, M., Hossain, R., Muldrey, B. J. & Hasan, S. Design of a low-overhead random number generator using CMOS-based cascaded chaotic maps. In *Proc. Great Lakes Symposium on VLSI*, 109–114 (ACM, 2021). https://doi.org/10.1145/3453688.3461504.
- [76] Wang, Z. et al. Optical frequency comb generation using CMOS compatible cascaded Mach-Zehnder modulators. IEEE J. Quantum Electron. 55, 1—6 (2019). https://doi.org/10.1109/JQE.2019.2948152.
- [77] Wang, Z. et al. On-chip frequency comb generation using cascaded MZMs in SiP for microwave photonics applications. In 2019 International Topical Meeting on Microwave Photonics (MWP), 1–3 (IEEE, 2019). https://doi.org/10.1109/MWP.2019.8892022.
- [78] Lin, J., Sepehrian, H., Xu, Y.-L., Rusch, L. A. & Shi, W. Frequency comb generation using a CMOS compatible SiP DD-MZM for flexible networks. *IEEE Photonics Technol. Lett.* 30, 1495–1498 (2018). https://doi.org/10.1109/LPT.2018.2856767.
- [79] Sharma, V. & Singh, S. Progress in optical frequency comb generation techniques towards flexible optical communication network. *J. Opt.* 27, 043001 (2025). https://doi.org/10.1088/2040-8986/adb1f2.

- [80] Dhakad, B. et al. Design and analysis of 16 channel WDM-OFC system with minimum ber for 5G applications. In Third International Conference on Communication, Networks and Computing CNC 2022, 28–39 (Springer, 2023). https://doi.org/10.1007/978-3-031-43140-1_4.
- [81] Yan, X., Zou, X., Pan, W., Yan, L. & Azaña, J. Fully digital programmable optical frequency comb generation and application. *Opt. Lett.* **43**, 283–286 (2018). https://doi.org/10.1364/OL.43.000283.
- [82] Arya, V., Kumari, M., Chauhan, R. & Sharma, N. Secure optical wireless satellite network based OWC-OCDM system with DDW code. In 2023 4th IEEE Global Conference for Advancement in Technology (GCAT), 1–5 (IEEE, 2023). https://doi.org/10.1109/gcat59970.2023.10353493.
- [83] Chan, V. Optical satellite network architecture. J. Opt. Commun. Netw. 16, A53–A67 (2023). https://doi.org/10.1364/jocn.499822.
- [84] Pan, R., Lin, G., Shi, Z., Zeng, Y. & Yang, X. The application of disturbance-observer-based control in breath pressure control of aviation electronic oxygen regulator. *Energies* 14, 5189 (2021). https://doi.org/10.3390/EN14165189.
- [85] Rehman, M. et al. RF sensing based breathing patterns detection leveraging USRP devices. Sensors 21, 3855 (2021). https://doi.org/10.3390/S21113855.
- [86] Khabbaz, A., Lampin, J.-F., Hindle, F. & Mouret, G. Molecular spectroscopy with a THz frequency comb. In 2024 49th International Conference on Infrared, Millimeter, and Terahertz Waves (IRMMW-THz), 1–2 (IEEE, 2024). https://doi.org/10.1109/irmmw-thz60956.2024.10697872.
- [87] Sterczewski, L. A., Bagheri, M. & Benmerabet, N. Cavity-enhanced Vernier spectroscopy with a chip-scale mid-infrared frequency comb. ACS Photonics 9, 994–1001 (2022). https://doi.org/10.1021/acsphotonics.1c01849.
- [88] Thorpe, M. J., Balslev-Clausen, D., Kirchner, M. S. & Ye, J. Human breath analysis via cavity-enhanced optical frequency comb spectroscopy. *Opt. Express* 16, 2387 (2007). https://doi.org/10.1364/OE.16.002387.
- [89] Jerez, B., Martín-Mateos, P., Prior, E., de Dios, C. & Acedo, P. Dual optical frequency comb architecture with capabilities from visible to mid-infrared. *Opt. Express* 24, 14986–14994 (2016). https://doi/10.1364/OE.24.014986.
- [90] Cundiff, S. T. & Ye, J. Colloquium: Femtosecond optical frequency combs. *Rev. Mod. Phys.* 75, 325 (2003). https://doi.org/10.1103/RevModPhys.75.325.
- [91] Long, D. A. et al. Nanosecond time-resolved dual-comb absorption spectroscopy. Nat. Photonics 1–5 (2023). https://doi.org/10.1038/s41566-023-01316-8.
- [92] Hu, H. & Oxenløwe, L. K. Chip-based optical frequency combs for high-capacity optical communications. *Nanophotonics* 10, 1367–1385 (2021). https://doi.org/10.1515/nanoph-2020-0561.
- [93] Lu, H.-H., Weiner, A. M., Lougovski, P. & Lukens, J. M. Quantum information processing with frequency-comb qudits. *IEEE Photonics Technol. Lett.* 31, 1858–1861 (2019). https://doi.org/10.1109/LPT.2019.2942136.
- [94] Chang, L., Liu, S. & Bowers, J. E. Integrated optical frequency comb technologies. *Nat. Photonics* **16**, 95–108 (2022). https://doi.org/10.1038/s41566-021-00945-1.
- [95] Tian, H. et al. Broadband, high-power optical frequency combs covering visible to near-infrared spectral range. Opt. Lett. 49, 538–541 (2024). https://doi.org/10.1364/OL.514182.